Aminodeoxychorismate Synthase Inhibitors from One-Bead One-Compound Combinatorial Libraries: "Staged" Inhibitor Design

Seth Dixon,[†] Kristin T. Ziebart,[†] Ze He,[‡] Melissa Jeddeloh,[†] Choong Leol Yoo,[†] Xiaobing Wang,[§] Alan Lehman,[§] Kit S. Lam,[§] Michael D. Toney,*[,†] and Mark J. Kurth*[,†]

Department of Chemistry, University of California, One Shields Avenue, Davis, California 95616, Department of Chemistry, Central Connecticut State University, 1615 Stanley Street, New Britain, Connecticut 06050, and Department of Internal Medicine, Division of Hematology and Oncology, UC Davis Cancer Center, 4501 X Street, Sacramento, California 95817

Received August 15, 2006

4-Amino-4-deoxychorismate synthase (ADCS) catalyzes the first step in the conversion of chorismate into *p*-aminobenzoate, which is incorporated into folic acid. We aim to discover compounds that inhibit ADCS and serve as leads for a new class of antimicrobial compounds. This report presents (1) synthesis of a mass-tag encoded library based on a "staged" design, (2) massively parallel fluorescence-based on-bead screening, (3) rapid structural identification of hits, and (4) full kinetic analysis of ADCS. All inhibitors are competitive against chorismate and Mg^{2+}. The most potent ADCS inhibitor identified has a K_i of 360 μM. We show that the combinatorial diversity elements add substantial binding affinity by interacting with residues outside of but proximal to the active site. The methods presented here constitute a paradigm for inhibitor discovery through active site targeting, enabled by rapid library synthesis, facile massively parallel screening, and straightforward hit identification.

Introduction

There is an ominous need for the discovery of fundamentally new classes of anti-infectives to fight the large-scale acquisition of bacterial and parasitic drug resistance. Historically, anti-infectives have been based mostly on natural product scaffolds, although some non-natural product based drugs are employed clinically (e.g., fluoroquinolones, sulfa drugs). The modern paradigm for discovery of new classes of non-natural product based drugs hinges on the meticulous choice of drug target and judicious attention to the molecular properties of drug candidates during their development. Intelligent combinatorial chemistry, wherein libraries are focused using knowledge of the structure of the target protein and restrictions on molecular properties, holds great promise for rapid lead discovery in anti-infective development.

Over the past decade, combinatorial chemistry and high-throughput screening have advanced greatly as tools in drug discovery.[1−3] With one-bead one-compound (OBOC) methods,[4−7] researchers have the tools to create vast libraries for discovery of biologically active compounds. However, difficulties still arise because of the sensitive nature of the solid support,[8] the challenges of synthesizing chemically unique structure-encoding tags,[9] the pitfalls of on-bead library testing,[10−14] and the structure decoding process.[9,15,16] Diverse methods must be brought together in a cohesive protocol to efficiently discover inhibitors using OBOC methods. For example, a library should be optimized by exploiting knowledge of the active/binding site. Additionally, a structure-encoding method must be implemented that accommodates the chemistry employed and that allows for the rapid and reliable identification of surface-bound ligands. Furthermore, elimination of false positives in on-bead screening is a necessity.

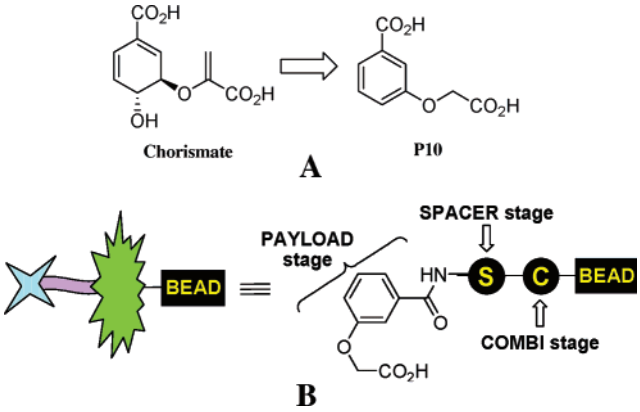

Figure 1. (A) Structure of chorismate and the chorismate-like inhibitor chosen for use in the test library synthesis. (B) Staged approach to our library design with the employed PAYLOAD derivative depicted.

Here, the target enzyme is 4-amino-4-deoxychorismate synthase (ADCS[a]), which has a rich history because of its potential as a target for antimicrobials.[17−21] Its substrate is chorismate (Figure 1A). Our library design incorporates a simple chorismate analogue (PAYLOAD) to give active site specificity connected through a SPACER to COMBI moieties. This "staged" design is inspired by the cholesterol-lowering statin drugs that inhibit hydroxymethylglutarate-CoA reductase. They contain a moiety structurally analogous to hydroxymethylglutarate coupled to ones that are completely unrelated to the cognate substrate.[22] Indeed, there is recent literature supporting this basic design strategy, which is grounded in multisubstrate analogue inhibitor theory.[23,24] Figure 1B illustrates this approach, where libraries are designed to exploit binding opportunities not only within

* To whom correspondence should be addressed. For M.D.T.: phone, 530-754-5282; fax, 530-752-8995; e-mail, mdtoney@ucdavis.edu. For M.J.K.: phone, 530-752-8192; fax, 530-752-8995; e-mail, mjkurth@ucdavis.edu.

[†] University of California.

[‡] Central Connecticut State University.

[§] UC Davis Cancer Center.

[a] Abbreviations: ADCS, 4-amino-4-deoxychorismate synthase; PLP, pyridoxal phosphate; ADCL, 4-amino-4-deoxychorismate lyase; LDH, lactate dehydrogenase; NADH, nicotinamide adenine dinucleotide, reduced form; IPTG, β-isopropylthiogalactoside; DCM, dichloromethane; DMF, dimethylformamide; DIEA, *N,N*-diisopropylethylamine; HOBt, *n*-hydroxybenzotriazole; DIC, diisopropylcarbodiimide; OBOC, one-bead one-compound.

10.1021/jm0609869 CCC: $33.50
Published on Web 11/10/2006

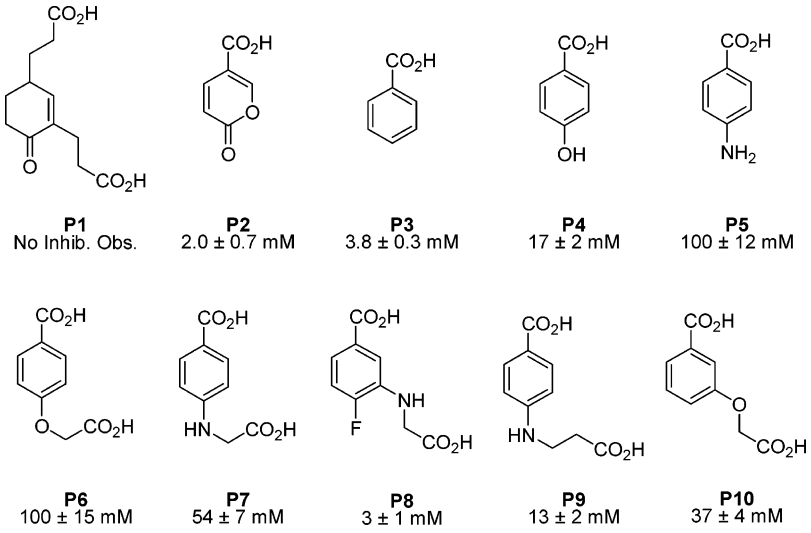

Figure 2. ADCS K_i values for potential PAYLOAD structures.

but also proximal to the ADCS active site. In the work reported here, the PAYLOAD (chorismate analogue) and SPACER stages (lysine) were held constant while the COMBI stage [acid−(lysine−PAYLOAD)−amino acid] was varied.

With this library design in mind, cyanogen bromide cleavable mass spectrum tags were chosen as a structure-encoding method for rapid identification of surface-presented molecules. Our previous experience with mass-tag encoded libraries nicely situated us for this work.[9,25] One concern with using encoding tags with on-bead screening is that they will interact with the target protein, leading to misidentification of the test compounds as the ligands. We were confident this would not be a problem using topologically segregated bifunctional beads because our recent work[16] demonstrated that the resin structure and the density of surface-bound ligands restrict proteins to the outside of the beads. Thus, confining the encoding tags to the bead interior exposes the protein only to surface ligands in on-bead assays.

Last, a facile method for high-throughput identification of ADCS-bound ("hit") beads is needed. On the basis of our previous experience, we decided to employ commercial, activated fluorescent dyes to label the surface of ADCS at lysine side chains.[26] This allows identification of ADCS-bound beads by manual observation under a fluorescence microscope or by automated COPAS (complex object parametric analyzer and sorter) sorting. Our original application of this technique was limited by background autofluorescence of random library beads, leading to false positives. Autofluorescence is a property inherent to all libraries we have studied and has been reported by others in the literature.[13,27] Therefore, automated COPAS sorting of the library *prior* to screening with fluorescently labeled ADCS was used to remove beads that autofluoresced. The COPAS instrument has the additional advantage of identifying the region of the spectrum that has the lowest amount of autofluorescence, allowing removal of the fewest beads from the library and selection of the most appropriate fluorescent dye.

A meaningful kinetic analysis of ADCS inhibitors requires an understanding of the enzyme's kinetic mechanism. ADCS requires Mg^{2+} for activity, which binds to the C1 carboxylate of chorismate and several active site glutamates at the solvent-exposed end of the active site. We therefore expected ADCS (and other homologous enzymes by extension) to obey an ordered kinetic mechanism with chorismate binding first and Mg^{2+} second. Initial rate kinetic data confirm this, as do fluorescence-quenching experiments with chorismate and staged inhibitors. Surprisingly, even simple chorismate analogues (as well as further elaborated inhibitors) are competitive against both chorismate and Mg^{2+}. This knowledge allowed us to show that PAYLOAD and PAYLOAD−SPACER inhibitors bind ∼60-fold weaker than chorismate and that the most potent inhibitor identified here binds ∼1.5-fold more tightly than chorismate.

With these tools now in place and our inhibitor design principle validated, focused libraries that include diversity structures more suited to ADCS inhibition can be produced. Most importantly, the methods reported here seamlessly bridge organic synthesis, combinatorial chemistry, and biological screening in a streamlined and cohesive protocol for the rapid discovery of biological ligands from highly diverse libraries.

Results

Design and Synthesis of the PAYLOAD and SPACER. Figure 2 depicts several PAYLOAD compounds that were considered for library synthesis. **P2**, **P3**, **P4**, and **P5** are available from commercial sources. **P6**,[28] **P7**,[29] and **P9**[30] were synthesized according to literature procedures. **P1** was synthesized according to procedures outlined in Scheme 1. Diels−Alder cycloaddition of the modified Danishefsky's diene (**P1a**) with methyl acrylate produced a diastereomeric mixture of cycloadducts (**P1b**). Exposure of these cycloadducts to a 10% HF−pyridine complex in acetonitrile led to a mixture of isomeric enones (**P1c** and **P1c′**). Vinylic alkylation of the enone mixture with methyl acrylate was expected to produce **P1d′**, which would deliver **P1′**, the actual target of this synthesis, upon ester hydrolysis. Exclusive formation of **P1d** occurred instead, resulting in synthesis of the revised PAYLOAD **P1**.

Scheme 2 describes the synthesis of **P8**. Reduction of **P8a** to **P8b** enabled N-alkylation with *tert*-butyl 2-bromoacetate to produce **P8c**. Subsequent saponification of **P8c** produced PAYLOAD **P8**. **P10** was chosen as the library PAYLOAD because of its ease in synthesis, simple adaptability to solid-phase synthesis, and its structural similarity to chorismate (i.e., a carboxylic acid containing side chain); its synthesis is described below and in Scheme 3.

For this proof-of-principle library, semiorthogonally protected lysine (i.e., Fmoc-Lys(Dde)-OH) was chosen as a framework on which to tether the PAYLOAD and COMBI stages. The carboxylic acid of the lysine was used in peptide bond formation with an amino acid diversity element, and the α-amine was

Scheme 1. Synthesis of **P1**[a]

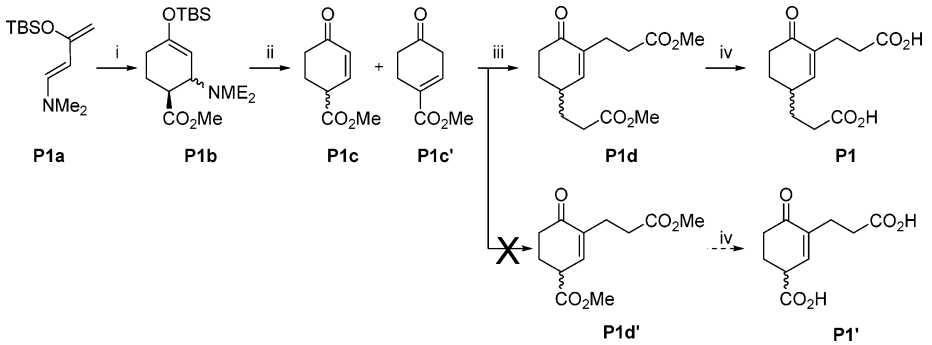

[a] Reagents and conditions: (i) methyl acrylate, toluene, room temp, 16 h; (ii) 10% HF/pyridine in CH_3CN, room temp, 2 h; (iii) methyl acrylate, DBU, DMF, reflux, 16 h; (iv) $Ba(OH)_2$, MeOH, room temp, 16 h.

Scheme 2. Synthesis of **P8**[a]

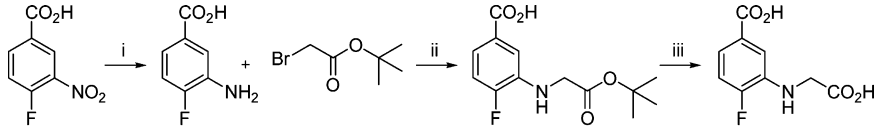

[a] Reagents and conditions: (i) H_2, Pd−C, EtOH, 16 h, room temp; (ii) TEA, THF, N_2, ∼50−60 °C, 16 h; (iii) TFA/DCM (1:1, v:v).

N-acylated with a carboxylic acid diversity element to deliver the COMBI stage. The ϵ-amine incorporated the PAYLOAD stage through N-acylation. The coupling strategy required that the aryl carboxylic acid of PAYLOAD **P10** be unprotected while the aryloxy acetic acid moiety is protected as a *tert*-butyl ester. As outlined in Scheme 3, the aryl acid moiety was protected as the methyl ester because it competed in the S_N2 displacement of bromide in the *tert*-butyl 2-bromoacetacetate alkylation step. O-Alkylation of this phenol (**1**) delivered **2**, and subsequent treatment with lithium hydroxide led to a mixture of the desired product **3** as well as 33% of the diacid **P10**. A sample of **P10** was saved for inhibition studies, and the remainder of **P10** was converted back into **3** by treatment with Boc-anhydride. This final conversion was carried out in high yield with complete selectivity for the aliphatic carboxylic acid.

Three other derivatives (**4**, **5**, and **7**) were synthesized to deconvolute the contributions of each inhibitor stage to binding. Compound **4** was synthesized from **3** using Rink amide resin. Compound **5** was synthesized to determine the contribution of the lysine SPACER to binding affinity. Solid-phase synthesis was again employed, giving **5** in high purity and good yield. Compound **7** was synthesized to determine if having a positively charged amino group near the normal position of the Mg^{2+} ion would enhance inhibitor binding. A reductive amination was performed on solid phase with **6**, the aldehyde analogue of **3**, to deliver **7** in high purity and good yield after a series of efficient steps.

Library Synthesis. The library used in this work was prepared as outlined in Scheme 4, using topologically segregated amino-functionalized resin. By employment of ∼90% of the total available functional groups for the encoding tag (restricted to the bead interior), strong MALDI-TOF tag signals were reliably detected.

Synthesis of the encoding tag was performed largely according to our published procedures.[9] The cleavable linker comprises four entities: (1) methionine, which enables resin cleavage by cyanogen bromide (methionine + cyanogen bromide → homoserine lactone);[31] (2) β-bromoalanine, which facilitates tag identification via bromine isotopic patterns in the mass spectrum;[32] (3) arginine; and (4) a linker. The last two increase tag solubility and molecular weight, which facilitates MALDI-TOF analysis by avoiding mass signals due to the matrix. The remaining transformations outlined in Scheme 4 completed construction of the coding tags and the target molecule found on the surface of the bead.

The protecting groups on the coding tag (Fmoc) and the surface of the bead (Alloc) were removed, and the first COMBI diversity element (amino acid X_1) was introduced. Next, the semiorthogonally protected lysine was attached to the growing coding tag and the target molecule. The beads were then swollen again in water for 24 h, and the outer surface and a fraction of the coding tag on the interior were protected with Fmoc (0.7 equiv), leaving the center of the bead with a free amine that was orthogonally protected with Boc. In this way, the innermost volume of the bead delivers a tag that reports the first COMBI diversity element (e.g., X_1).

The second COMBI diversity element was introduced after Fmoc deprotection. PAYLOAD **3** was then coupled to the Dde-deprotected distal amine. The second coding tag contained the complete target molecule. The entire surface target molecule could then be identified by MALDI-TOF after CNBr cleavage of the coding tags from the resin. PAYLOAD **3** coupling and removal of all protecting groups completed the MS-encoded library synthesis. The incorporation of 48 amino acid diversity elements for X_1 and 48 carboxylic acid diversity elements for X_2 resulted in 2304 test compounds.

Identification of each diversity element was accomplished with the following equations:

$$X_1 = M_1 - 712 - (\text{K coupled with } \mathbf{P10})$$

$$X_2 = M_2 - M_1 - 712 - (\text{K coupled with } \mathbf{P10})$$

In these equations, M_1 and M_2 are MALDI-TOF mass signals corresponding to the first and second tag signals that each display a signature bromine isotopic pattern. As a test, several beads were removed from the library during synthesis and sequenced to validate the library synthesis. These beads delivered the expected MALDI-TOF signals at each test point. These spectra are supplied in the Supporting Information.

Scheme 3. Synthesis of **P10** and Other Derivatives[a]

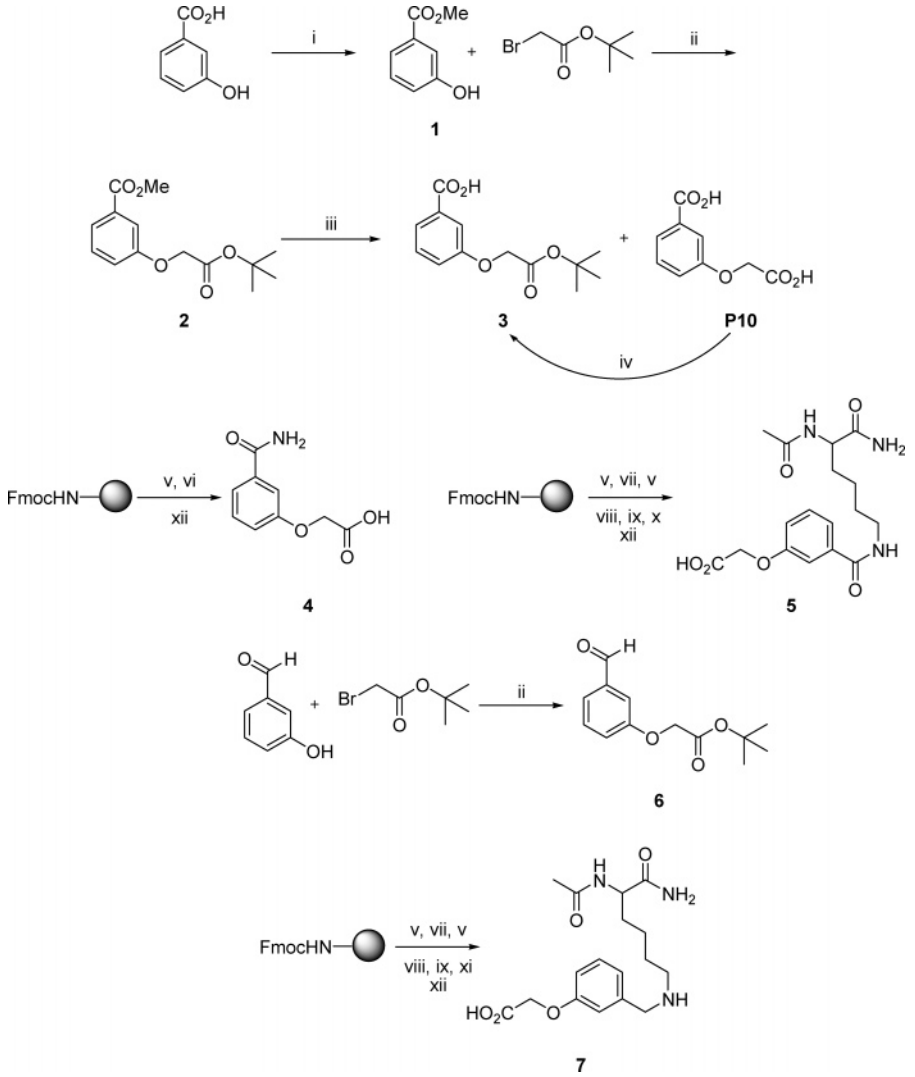

[a] Reagents and conditions: (i) AcCl, MeOH, N_2, reflux, 8 h; (ii) K_2CO_3, THF, N_2, 4 h; (iii) LiOH, H_2O, THF, 6 h; (iv) $(Boc)_2O$, DMAP, CH_3CN, N_2, 0 °C, room temp, 16 h; (v) 20% piperidine in DMF, 2 × 10 min; (vi) **3**, HOBt, DIC; (vii) Fmoc-Lys(Dde)-OH, HOBt, DIC; (viii) acetic anhydride (10 equiv), DIEA (12 equiv), DMF; (ix) 2% hydrazine in DMF, 2 × 10 min; (x) **2**, HOBt, DIC; (xi) **6**, $NaCNBH_3$, 1% AcOH, TMOF; (xii) TFA/$H_2$0/TIS (95, 2.5, 2.5, v/v/v).

COPAS Sorting of the Library. In our and others' experience, combinatorial libraries created using OBOC methods with aromatic compounds contain beads that autofluoresce. Therefore, this library was presorted to remove strongly autofluorescent beads prior to screening with fluorescently labeled ADCS. This presort established which region of the fluorescence spectrum exhibited the most autofluorescence and helped define which fluorescent dye would incur the least intereference in the fluorescent-based screening. Relative to a defined baseline, the red and green regions of the spectrum exhibited 15% and 5% autofluorescence, respectively. Autofluorescence was more frequent but less intense in the red region and more intense and less frequent in the green region. Therefore, the sort was performed in the green region such that the number of eliminated beads was minimized. The results of the presorting are shown in Figure 3; the original library contained autofluorescing beads that the COPAS instrument effectively removed (see Figure S1 in the Supporting Information).

Screening of the Library. The Alexa Fluor 488 labeled enzyme exhibited 84% of the activity of the unlabeled enzyme, as determined from the LDH-coupled assay (vide infra). After a 1 h incubation with labeled enzyme, the library was viewed under a fluorescence microscope in 15 batches of ~2500 beads each. In each batch, ~2% of the beads that strongly fluoresced were isolated manually with a micropipette; of these, 15 of the brightest fluorescing beads were selected. The "hit" beads were washed with 8 M guanidine hydrochloride (to remove ADCS) and water.

MALDI-TOF Analysis and Resin-Free Resynthesis. Each of the washed "hit" beads was individually incubated with cyanogen bromide to cleave the tags. MALDI-TOF analysis produced signals that allowed surface ligand identification for 11 of the 15 washed and cleaved "hit" beads. This corresponds to 73% readability, which is in accord with literature values.[33] The 11 compounds identified by the MALDI-TOF are shown in Figure 4. As a representative example, the spectrum used to identify **L2** is shown in Figure 5. Additional examples are given in the Supporting Information. From these results, two sets of duplicate ligands (**L1** = **L4**; **L3** = **L8** = **L11**) were found, suggesting that the majority of the library had been screened and that the ligands identified were among the tightest binding. These ligands exhibit a distinct structural pattern, with each containing a hydrophobic and hydrophilic group in the COMBI stage. The ligands were resynthesized on-bead using Rink amide resin and released for kinetic analysis. The resynthesized ligands were purified to >95% by HPLC.

Scheme 4. Synthesis of MS-Encoded Library[a]

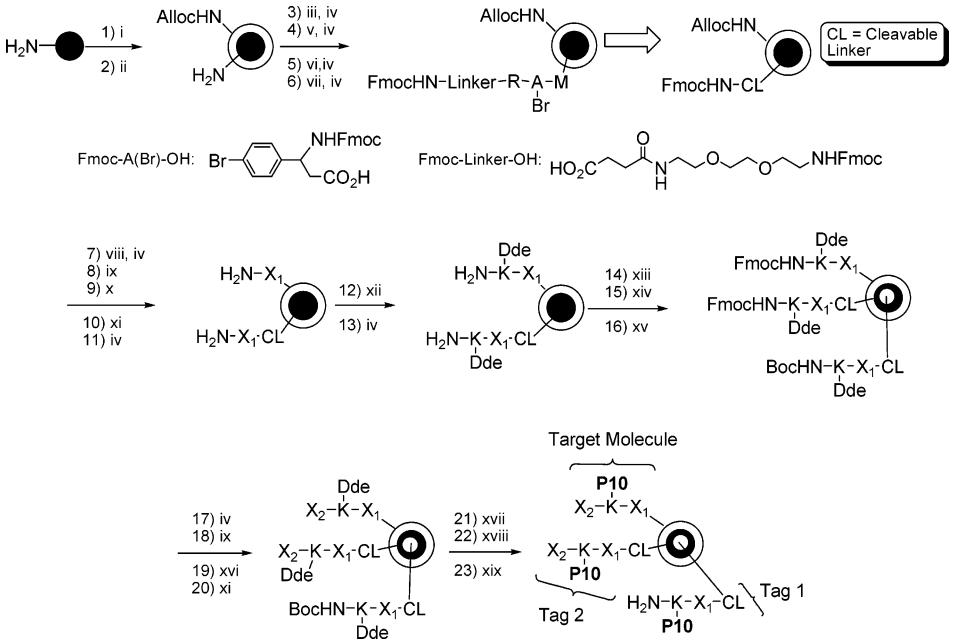

[a] Reagents and conditions: (i) H_2O, 48 h; (ii) Alloc-OSu (0.1 equiv), DIEA, DCM/Et_2O (55:45, v:v), 30 min; (iii) Fmoc-Met-OH, HOBT, DIC; (iv) 20% piperidine in DMF, 2 × 10 min; (v) *N*-Fmoc-3-(4-bromophenyl)-β-alanine, HOBt, DIC; (vi) Fmoc-Arg(Pmc)-OH, HOBt, DIC; (vii) *N*-Fmoc-2,2′-ethylenedioxybis(ethylamine)monosuccinamide, HOBt, DIC; (viii) $Pd(PPh_3)_4$ (0.24 equiv), $PhSiH_3$ (20 equiv), DCM; (ix) split beads into 42 columns; (x) library assembly (Fmoc-X_1-OH, HOBt, DIC); (xi) mix beads; (xii) Fmoc-Lys(Dde)-OH, HOBt, DIC; (xiii) H_2O, 24 h; (xiv) Fmoc-Osu (0.7 equiv), DIEA, DCM/Et_2O (55:45, v:v), 1 h; (xv) $(Boc)_2O$ (1 equiv), DIEA, DCM; (xvi) library assembly X_2-CO_2H, DIC, HOBt; (xvii) 2% hydrazine in DMF; (xviii) 3-(2-*tert*-butoxy-2-oxoethoxy)benzoic acid (**3**), HOBt, DIC; (xix) TFA/phenol/TIS/H_2O/ethanedithiol (90/5/2/2/1, v/w/v/v/v).

Kinetic Results. Initial rate data for determining the kinetic mechanism of ADCS were obtained by measuring the increase in absorbance at 290 nm due to PABA formation in a coupled assay with excess ADCL. Figure 6A shows the results of these experiments; the data fit best to the equation for an ordered sequential mechanism, with chorismate binding first:

$$v_i = \frac{V_{max}[\text{chorismate}][Mg^{2+}]}{K_{\text{chorismate}}K_{Mg^{2+}} + K_{Mg^{2+}}[\text{chorismate}] + [\text{chorismate}][Mg^{2+}]} \quad (1)$$

The data in Figure 6A provided initial estimates of the kinetic constants $K_{\text{chorismate}}$ and $K_{Mg^{2+}}$. More accurate estimates were obtained from experiments in which the concentration of one substrate was varied across a wide range while the other was held constant at its estimated K_M value. This gave $K_{\text{chorismate}} = 0.50 \pm 0.05$ mM and $K_{Mg^{2+}} = 10 \pm 1$ μM.

Each inhibitor was assayed against ADCS by varying the inhibitor concentrations across an appropriate range and holding the chorismate concentration constant at 13 μM (the K_M value under the assay conditions). Strong absorbance below 300 nm due to the inhibitors necessitated the use of a second coupling enzyme, LDH. Initial rates were measured by following the decrease in absorbance at 340 nm due to NADH oxidation. The data were fitted to the following competitive inhibition equation:

$$v_i = \frac{V_{max}[\text{chorismate}]}{K_M\left(\frac{[I]}{K_i}\right) + [\text{chorismate}]} \quad (2)$$

As justification for this fit, **P9**, **P10**, **4**, **5**, **7**, and **L5** were subjected to further kinetic analysis, wherein inhibitor and chorismate concentrations were each varied. Lineweaver−Burk analysis of the data revealed each compound to be a competitive inhibitor of ADCS. The data obtained for **P10** are depicted in Figure 6B as a representative example. Kinetic analyses were performed for all identified ligands. All have lower K_i values relative to **P10** (Figure 2).

Surprisingly, compounds **P10**, **4**, **5**, and **L5** were all found to be competitive with respect to Mg^{2+} as well as chorismate. As a representative example, Figure 6C illustrates the data obtained for **P10**. The LDH-coupled assay was used. Inhibitor and Mg^{2+} were varied across appropriate concentrations, while chorismate was held constant at 200 μM.

Discussion

The increase in drug-resistant pathogenic microorganisms and the near-abandonment of antimicrobial drug development by the pharmaceutical industry make the involvement of academia in this pursuit a pressing priority. The success of academic efforts will hinge on creative methods development that enables discovery with substantially less manpower than that available to companies. An obvious basis on which to choose drug targets is their essentiality to microbial survival and their absence in humans. Herein, the development of facile, powerful methods for readily automatable massively parallel screening of OBOC combinatorial libraries has been described in application to the discovery of ADCS inhibitors, this enzyme and its homologues being critical to microbial survival as well as being absent in mammals.

The shikimate pathway converts glucose into chorismate, the branch-point metabolite for carbocyclic aromatic compound biosynthesis in biological systems. Five primary metabolic pathways start from chorismate (Phe/Tyr, salicylate/siderophores, PABA/folates, Trp, and electron-transfer quinones), while several secondary metabolites also begin with chorismate.[18] These pathways, including the shikimate pathway itself, are absent in humans; their products are essential components

Figure 3. COPAS sorts of beads based on autofluorescence: (A) first sort of the target library in which 12 541 beads were sorted in the batch shown, with 6.0% beyond the user-defined threshold (black line in plot); (B) second sort of the target library in which 7735 beads were sorted in the batch shown, with 4.0% of the beads above the threshold; (C) third sort of the target library in which 21 118 beads were sorted in the batch shown, with less than 1.0% above the threshold. Blue, green, and red dots represent the occurrence of 100, 10, and 1 beads, respectively, in the same location. The red circles are added to focus attention on these regions of the plots, which highlight the removal of green-fluorescing beads.

of our diet. The attractiveness of these pathways as antimicrobial targets has long been recognized.[19,20] Several effective present day commercial compounds/drugs act on these pathways, including the commercial herbicide glyphosate, the sulfa drugs, and others.

ADCS, anthranilate synthase, and isochorismate synthase are three structurally and mechanistically homologous chorismate-utilizing enzymes that initiate PABA, Trp, and salicylate biosynthesis, respectively. Our antimicrobial drug discovery goal is to find a compound that is a tight-binding inhibitor of one or more of these three similar enzymes, since each pathway is critical to bacterial pathogenicity.[34,35] A compound that inhibits more than one will have a radically reduced likelihood that primary resistance by simultaneous mutation of two or more of these enzymes will develop. It would be equivalent to a multidrug cocktail in a single inhibitor molecule. The high degree of similarity between these enzymes makes this lofty goal a reasonable pursuit. We report inhibition studies targeting ADCS here. Efforts targeting anthranilate synthase and isochorismate synthase will be undertaken in due course.

Given this stated goal, we decided that, rather than optimize a single small substrate-like molecule for tight inhibition of two or more of these enzymes, a more generalized strategy would have a higher probability of success. The structures of these enzymes all show that the active sites are removed from solvent but not extraordinarily deeply buried in the protein interior. While we pondered the structures, the popular cholesterol-lowering statin drugs came to mind because these varied compounds all have a substrate-like moiety that directs them to the active site. This substrate-like moiety does not give tight binding but is connected by a "linker" moiety to a group of structurally diverse moieties, each of which is unique to a given drug. This latter component makes serendipitous interactions with the enzyme proximal to the active site and contributes the greatest portion of the binding energy of these tight-binding hydroxymethylglutarate-CoA inhibitors.[22] We reasoned that a similar strategy might be the most productive for finding a single compound that inhibits one or more of ADCS, AS, and IS.

We have termed the tripartite inhibitor design employed here a "staged" design in which there is an active site-directing PAYLOAD stage, a SPACER stage that extends out of the active site, and a COMBI stage that is the focus of the combinatorial chemistry employed here and that is expected to make productive binding interactions with the enzyme surface proximal to the active site.

The first task was to find a stable chorismate analogue that would be easily amenable to solid-phase synthesis and would direct the inhibitor library to the active site. On the basis of previous inhibition studies by others, a side chain containing a carboxylate group linked through one or two carbons was essential for tight binding to IS and AS.[36,37] To this end, we surveyed the compounds presented in Figure 2 as possible candidates. **P10** was chosen as the best compromise between all of these requirements.

The second component in our design is the SPACER. In the full embodiment of our discovery efforts, this moiety will be the target of diversification and optimization through combinatorial chemistry and screening with labeled enzyme. For this initial proof-of-principle demonstration, we decided to simplify matters and use lysine as the SPACER; modeling showed that it is an excellent first approximation to the length required to extend out of the active site to the surface cleft, where the COMBI moiety would have opportunities for serendipitous interactions with residues near the surface (see Figure S2 in the Supporting Information). Lysine also contains the α-amino and α-carboxylate functional groups that are readily amenable to solid-phase elaboration with the combinatorial elements.

A series of 48 acids were chosen as diversity elements for acylation of the α-amine and a series of 48 amino acids were chosen as diversity elements for coupling to the α-carboxylate of lysine, leading to our proof-of-principle one-bead one-compound library of 2304 compounds. Encoding of the structures was achieved with a mass spectrum tagging scheme using topologically segregated resin beads, described in detail above, which allowed rapid and facile test compound structure identification (Figure 5).

With the library in hand, we first presorted it using the COPAS instrument to increase the signal-to-noise for hit compounds by removing the autofluorescing beads that interfere with identification of ADCS-bound beads (Figures 3 and S1). This presorting had a major impact on our ability to identify ADCS-bound beads with a low false-positive frequency, since 6% of the beads were removed in the presort and ~2% of the presorted beads incubated with labeled ADCS were fluorescent.

Figure 4 shows 11 structures obtained from the 15 brightest beads picked in the ADCS screen. These were resynthesized

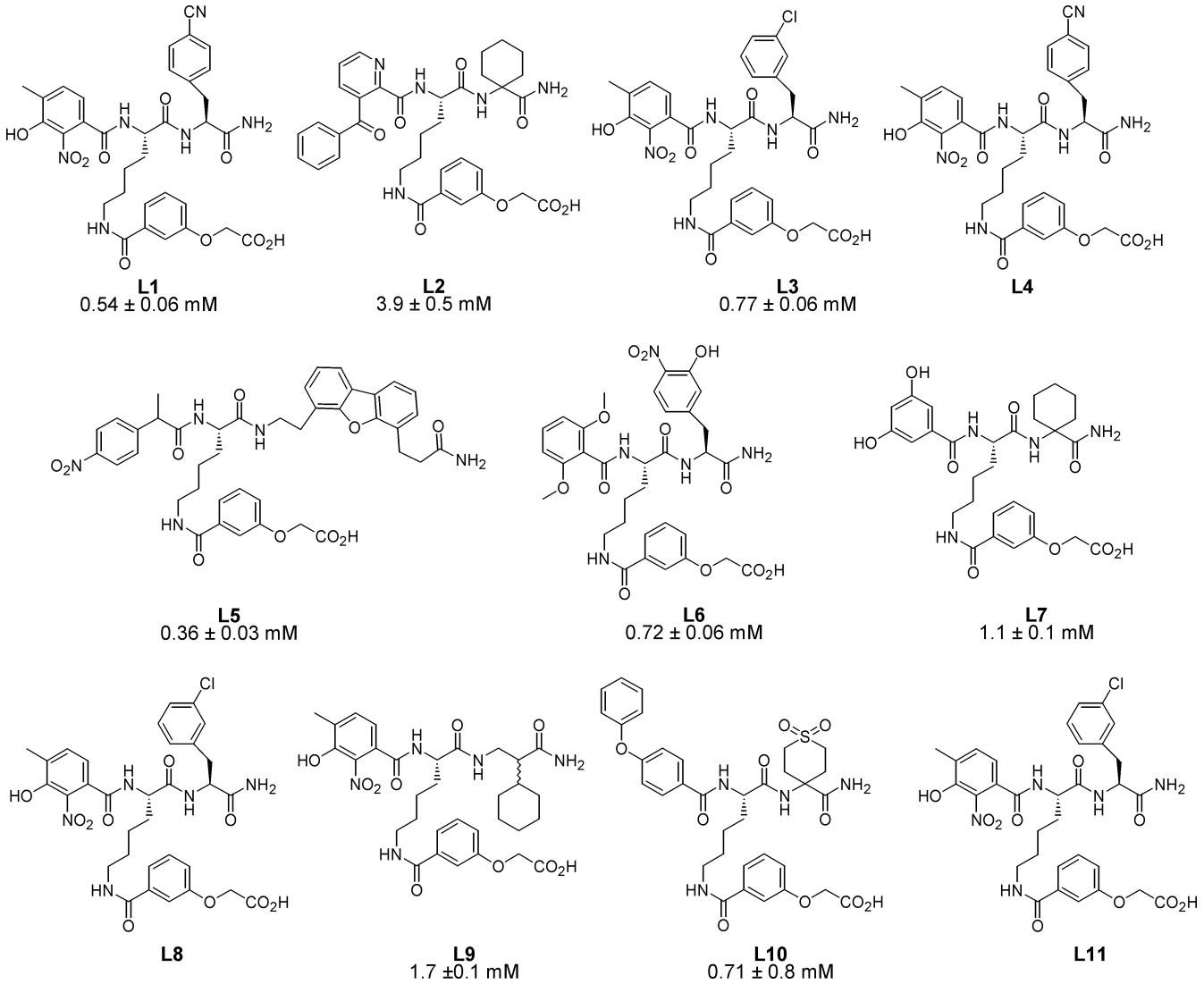

Figure 4. K_i values for ligands identified from the Alexa Fluor 488 labeled ADCS screen. **L1** and **L4** are identical structures, as are **L3**, **L8**, and **L11**.

on Rink amide resin, and the inhibition constants of those sufficiently soluble to assay are reported under the structures. These compounds are not tight binding by any standard, but they serve the very important role of demonstrating that the "staged" inhibitor design is a promising line of pursuit. Each of the staged inhibitors assayed has a substantially lower inhibition constant than **P10**, indicating that the SPACER and/or COMBI moieties provide significant increases in binding affinity.

The tightest binding inhibitor identified is **L5** with a K_i value of 360 μM. We designed and synthesized the derivatives shown in Figure 7 to deconvolute the contributions to binding affinity by the various components. Surprisingly, the conversion of **P10** into its simple amide (**4**) had no significant effect on binding affinity. This important point is addressed below in relation to the kinetic mechanism of ADCS. Additional elaboration by formation of the amide with the ϵ-amino group of *N*-acetyl-L-lysine amide (**5**) also does not significantly alter the binding affinity of the **P10**-based inhibitor, demonstrating that any potential negative interactions between the lysine and the enzyme are offset by positive ones and more importantly that all of the interactions that lead to the ~100-fold increase in binding affinity of **L5** compared to **P10** are entirely due to interactions made between the COMBI moiety and the enzyme surface proximal to the active site.

The kinetic mechanism of ADCS has not been characterized in the literature. It is important for our analyses here to understand whether chorismate and Mg^{2+} binding obeys a random or ordered sequential mechanism so that the effect of their concentrations on inhibitor binding can be ascertained. Our results show that ADCS obeys a strictly ordered kinetic mechanism with chorismate binding first and Mg^{2+} second:

$$\mathrm{E} + \text{chorismate} \underset{}{\overset{K_{\text{chorismate}}}{\rightleftharpoons}} \mathrm{E}\cdot\text{chorismate} \underset{\mathrm{Mg}^{2+}}{\overset{K_{\mathrm{Mg}^{2+}}}{\rightleftharpoons}}$$

$$\mathrm{E}\cdot\text{chorismate}\cdot\mathrm{Mg}^{2+} \xrightarrow{k_{\text{cat}}} \mathrm{E} + \mathrm{ADC} + \mathrm{Mg}^{2+}$$

Full inhibition analyses of several inhibitors including **P10**, **4**, **5**, and **L5** show that they are all competitive with respect to *both* chorismate and Mg^{2+}. The results for **P10** are shown in Figure 6B. This was expected for the latter compounds but not for **P10**. It is a close analogue of chorismate, whose C1 carboxylate group is a bidentate ligand to Mg^{2+} in the active enzyme complex.[38]

Given that **P10** is structurally different enough from chorismate to preclude Mg^{2+} binding, then the correct comparison for binding is not to chorismate in the ternary complex with enzyme and Mg^{2+} but rather to chorismate in the binary complex with enzyme alone. This value, $K_{\text{chorismate}}$ in the ordered kinetic

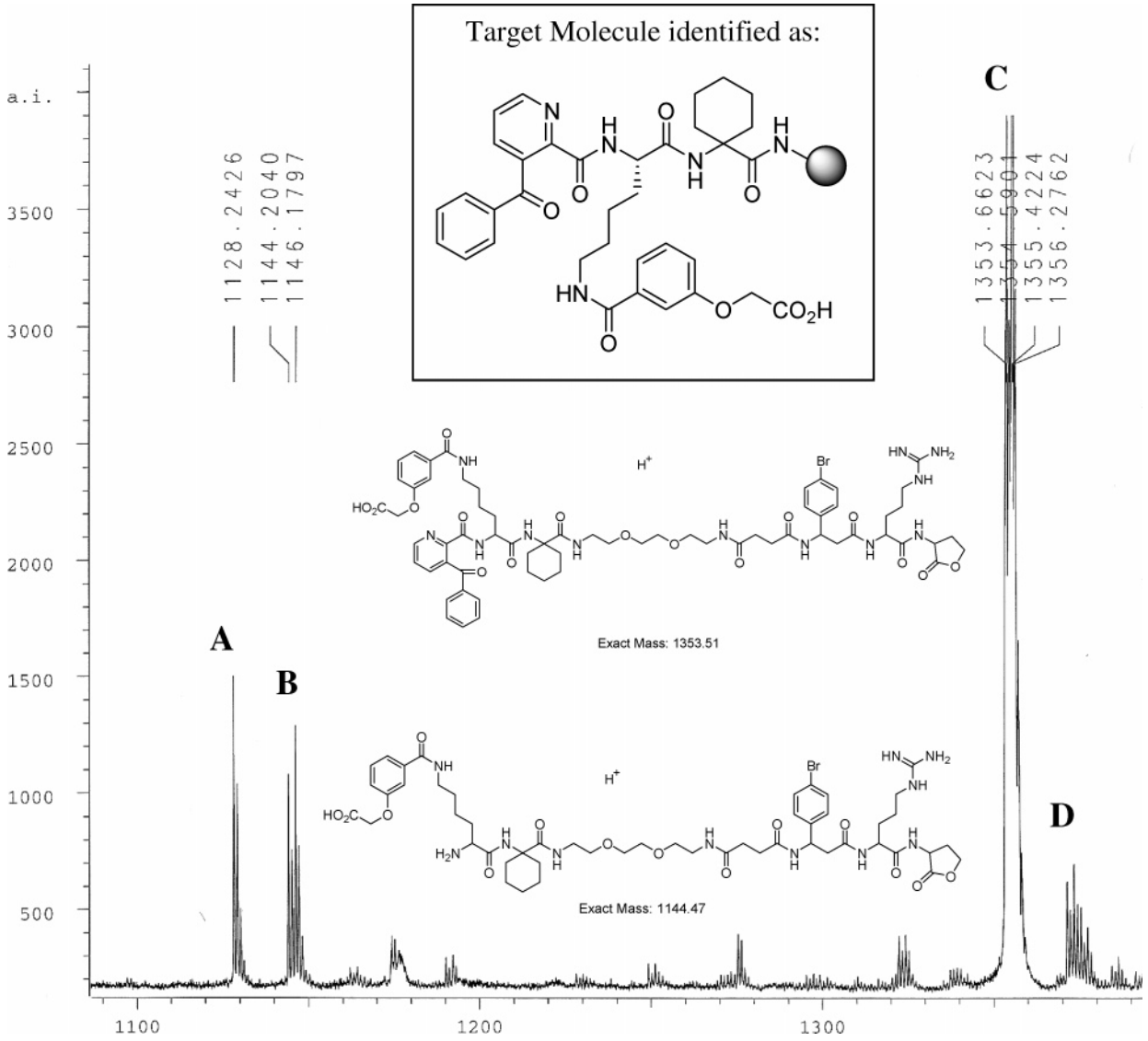

Figure 5. Example MALDI-TOF spectra obtained from an ADCS-selected hit bead. Each major peak exhibiting a monobromine splitting pattern was used to calculate the diversity element present; the diversity structure determined is shown with the cleavable linker. Peak A is the mass signal of a peptide fragment without the bromine component. Peak B is the mass signal used to calculate tag 1. Peak C is the mass signal used to calculate tag 2, and peak D is the mass signal associated with a formylated tag 2.

mechanism, was determined here to be 0.5 mM, much larger than the value of 13 μM previously measured for chorismate in the presence of 5 mM Mg^{2+}.[39] Therefore, **P10** binds only ~60-fold more weakly than chorismate to give the equivalent enzyme complex. Competitive inhibition with respect to both chorismate and Mg^{2+} by simple chorismate analogues with ADCS but not with anthranilate synthase or isochorismate synthase may explain previous inhibition studies that showed that chorismate analogues generally bind more tightly to the latter two compared to ADCS in the presence of Mg^{2+}.[37,40]

The competitive inhibition of **P10** with respect to *both* chorismate and Mg^{2+} also provides a satisfying explanation for why conversion of **P10** to its amide **4** does not drastically increase the inhibition constant. Conversion of the carboxylate group to the amide would be expected to disrupt the energetically favorable Mg^{2+} binding if **P10** did, in fact, allow Mg^{2+} to bind. The observation that conversion to the simple amide has an insignificant energetic effect is additional evidence that Mg^{2+} does not bind to the ADCS−**P10** complex. Furthermore, this also suggests that the negative charge of the aryl carboxylate group of **P10** does not contribute significantly to its binding (or that the amide group provides for energetically equivalent interactions).

The similar K_i for **5** compared to **P10** and **4** implies that the lysine SPACER moiety incurs neither good nor bad interactions (or they are equal) with the enzyme as it traverses the Mg^{2+} binding site to the enzyme surface. This positive result demonstrates that the steric bulk of the linker is readily accommodated. The lysine SPACER used here was chosen for synthetic facility. A combinatorial effort aimed at optimizing the PAYLOAD−SPACER combination has the potential to generate substantial binding energy from the SPACER moiety given several glutamates (which form most of the Mg^{2+} binding site) and other polar groups in this region. Retrospectively, an initial effort was made to capture some of this binding energy by synthesizing **7**. It was disappointing to find that conversion of the amide of **5** to the benzylamine of **7** did not generate substantial additional binding interactions. This may well be due to the suboptimal position of the positively charged amino group that was intended to capture some of the binding energy Mg^{2+} enjoys. It is likely that SPACER optimization through a non-peptide-based combinatorial program will remedy this.

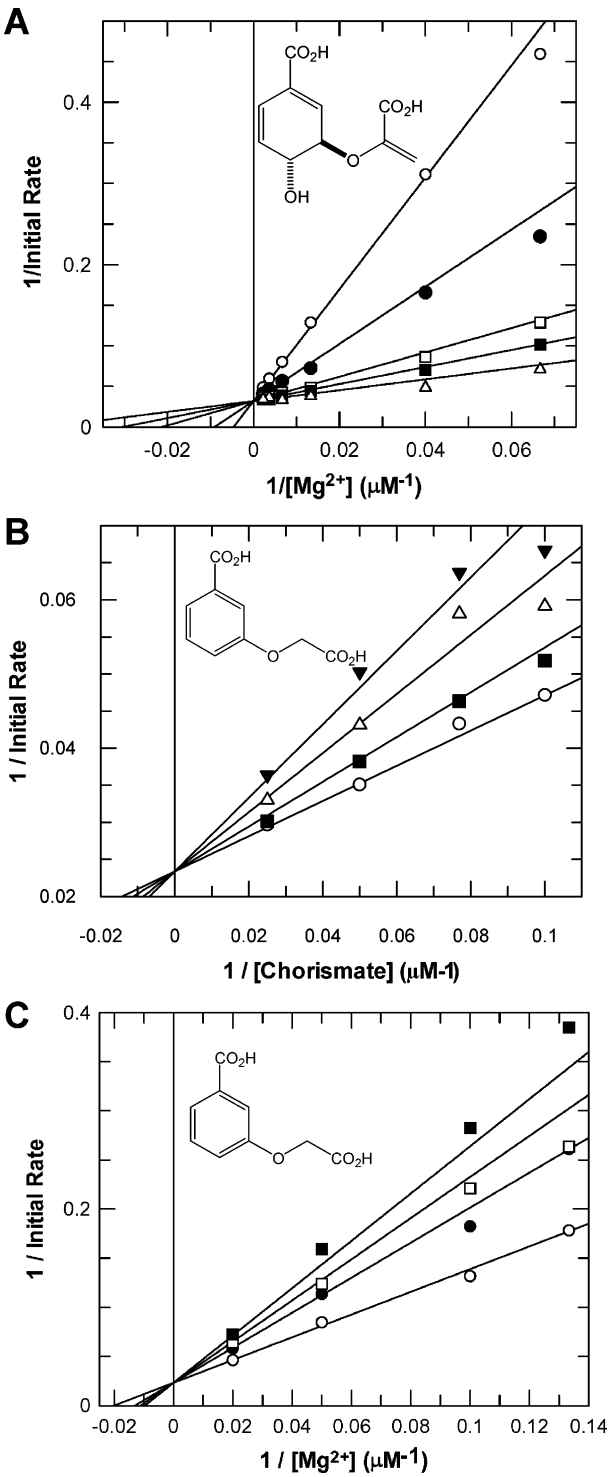

Figure 6. Kinetic analyses of ADCS. The structures of the compounds whose concentrations were varied along with those indicated on the *X*-axes are shown in the figures. (A) Double-reciprocal plot showing the effect of Mg^{2+} upon chorismate binding. This and other data (not shown) definitely demonstrate that the kinetic mechanism for ADCS is ordered, with chorismate binding first and Mg^{2+} second. The concentrations of chorismate are 50, 100, 250, 375, and 650 μM. (B) Double-reciprocal plot showing that **P10** is competitive against chorismate. The concentrations of **P10** are 0, 10, 25, 40 mM. (C) Double-reciprocal plot showing that **P10** is competitive against Mg^{2+}. The concentrations of **P10** are 0, 15, 22.5, 30 mM.

Last, the effect of the resin linker on the affinity of ADCS for resin-bound test compounds was delineated. Figure 7 presents the structures of **L3** and **L5** derivatives where a close structural analogue of the resin linker is attached to the carboxylate used for resin attachment. For both **L3** and **L5** the inclusion of the linker analogue had only a minor effect on the affinity of the test compound for ADCS. This gratifying result demonstrates that covalent attachment of the test compound to the resin through the linker has negligible deleterious effects on the affinity of the enzyme for it.

This work has demonstrated the viability of a general paradigm for drug discovery based on combinatorial chemistry and a "staged" inhibitor design. A great majority of enzymes bind their substrates in an active site that is close to the surface of the protein and have an open channel that leads to solvent. A substrate-like moiety that directs a molecule to an enzyme active site, even if it alone has a relatively low affinity, can be elaborated to take advantage of serendipitous interactions that can lead to high affinity. The use of fluorescently labeled enzyme to detect binding to surface-bound test compounds ultimately enables full automation of this simple screening procedure by COPAS-based presorting of the library followed by sorting of the enzyme binding reactions in which beads become fluorescent because of enzyme association to surface ligands.

Materials and Methods

Reagent and Instrumentation. All reagents and solvents were purchased from commercial suppliers and used without further purification. TentaGel S NH_2 resin (90 μm, 0.26 mmol/g) was purchased from Rapp Polymere GmbH (Tübingen, Germany), and all the calculations for synthesis were based on a substitution of 0.26 mmol/g. Fmoc-protected amino acids were purchased from Chem-Impex International, Inc. (Wood Dale, IL) and Advanced ChemTech (Louisville, KY). *N*-Fmoc-3-(4-bromophenyl)-β-alanine was purchased from InnovaChem (Tuscon, AZ). *N*-Fmoc-2,2′-ethylenedioxybis(ethylamine)monosuccinamide was synthesized according to literature procedure.[25] HOBt, Fmoc-OSu, and DIC were purchased from GL Biochem (Shanghai, China). Alexa Fluor 488 succinimidyl ester was purchased from Invitrogen (Molecular Probes). Fmoc Rink amide MHBA resin (capacity, 0.65 mmol/g) was purchased from Nova Biochem. Melting points are uncorrected. All infrared spectra were determined on a Genesis II Mattson FT-IR. ^1H and ^{13}C NMR were measured in either DMSO-d_6 or $CDCl_3$ at 400 (or 300) and 100 (or 75) MHz, respectively. Elemental analyses were determined at MidWest Microlab, Indianapolis, IN. MALDI-TOF MS analyses were performed with a Bruker Biflex III MALDI-TOF mass spectrometer (Bruker-Franzen Analytik, Bremen, Germany) equipped with a pulsed N_2 laser (337 nm), a delayed extraction ion source, and a reflectron. Waters Alliance LC/MS, equipped with a Waters 2695 HPLC and a Waters PDA 996, was used for HPLC purity analyses employing a gradient elution of 0−100% B over 30 min, monitored from 200 to 400 nm. A Waters Micromass ZQ mass detector was used in ESI MS for the identification of various products, with a product concentration of 1 μg/mL. Further analytical HPLC was performed on a System Gold 125 solvent module (Beckman) with a C_{18} column (Vydac, 5 μM, 4.6 mm i.d. × 25 cm). A gradient elution of 0−80% solvent B over 25 min followed by 80−100% solvent B over 3 min was used at a flow rate of 1 mL/min (solvent A is H_2O/0.1% TFA; solvent B is acetonitrile/0.1% TFA). Preparative HPLC was performed on a System Gold 126NMP solvent module (Beckman) with a C_{18} column (Vydac, 5 μM, 2.5 cm i.d. × 25 cm). A gradient elution of 0−60% solvent B over 25 min followed by 60−100% solvent B over 25 min followed by 100% solvent B for 5 min was used at a flow rate of 7 mL/min (solvent A is H_2O/0.1% TFA; solvent B is acetonitrile/0.1% TFA). The COPAS sorter was purchased from Union Biometrica (Somerville, MA).

Synthesis of Methyl 3-hydroxybenzoate (1). *m*-Hydroxybenzoic acid (10.0 g, 72.5 mmol) was dissolved in methanol (70 mL), and the solution was placed under nitrogen and cooled in an ice bath. Acetyl chloride (7.2 mL, 7.96 g, 101.4 mmol) was added via

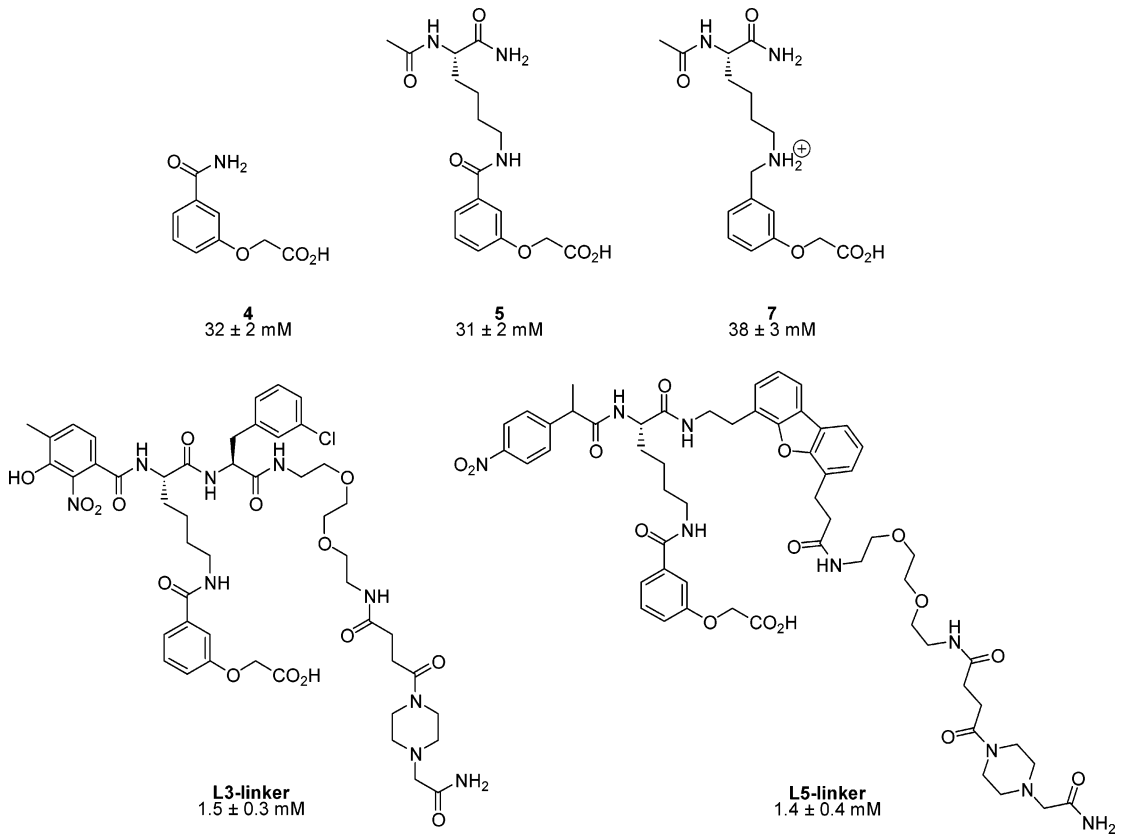

Figure 7. Structures and K_i values for inhibitor elaborations and derivatives.

syringe. The reaction mixture was removed from the ice bath and then heated to reflux in an oil bath for 8 h, after which the solvent was removed by rotary evaporation. The resulting solid was dissolved in water (50 mL) and extracted with ethyl acetate (3 × 50 mL). The combined organic layers were dried with $MgSO_4$ and concentrated by rotary evaporation. Crude product (**1**) was used without further purification; yellow solid (10.65 g, 93.7% crude yield, purity ∼99%). MS (ESI) *m/z*: 152.02 [M^+]. ^{1}H NMR (DMSO-d_6): δ 9.83 (s, 1H), 7.39 (m, 3H), 7.16 (m, 1H), 3.83 (s, 3H).

Synthesis of Methyl 3-(2-*tert*-Butoxy-2-oxoethoxy)benzoate (2). Compound **1** (5.0 g, 32.7 mmol) was dissolved in THF (70 mL), and to this solution was added K_2CO_3 (13.5 g, 98.0 mmol). The mixture was placed under nitrogen and allowed to stir for 1 h and then cooled in an ice bath. *tert*-Butyl 2-bromoacetate (3.96 g, 39.2 mmol) was added via syringe. The solution was removed from the ice bath and warmed to room temperature at which time TLC indicated the reaction had gone to completion. The solvent was removed by rotary evaporation. The resulting solid was dissolved in water (50 mL) and extracted with ethyl acetate (3 × 50 mL). The combined organic layers were dried with $MgSO_4$ and concentrated by rotary evaporation. The crude product (**2**) was used without further purification as a yellow solid (8.39 g, 96.7% crude yield, purity ∼94%). MS (ESI) *m/z*: 266.71 [M^+]. ^{1}H NMR (DMSO-d_6): δ 7.59 (d, J = 2.7, 1H), 7.43 (m, 2H), 7.23 (d, J = 2.4, 1H), 4.79 (s, 2H), 3.84 (s, 3H), 1.44 (s, 9H).

Method A: Synthesis of 3-(2-*tert*-Butoxy-2-oxoethoxy)benzoic Acid (3) and 3-(Carboxymethoxy)benzoic Acid (P10). Compound **2** (17.88 g, 67.2 mmol) was dissolved in THF/water (1:1, 50 mL), and to this stirring solution was added LiOH (3.10 g, 73.9 mmol). This solution was stirred at room temperature until TLC showed the disappearance of **2**, at which time the THF was removed by rotary evaporation and the pH of the remaining aqueous solution was adjusted to between 2 and 3 with 1 M HCl. This acidic solution was extracted with ethyl acetate (3 × 50 mL), and the combined organic layers were dried over $MgSO_4$ and concentrated by rotary evaporation. The crude product was subjected to silica gel column purification with 3:1 *n*-hexane/ethyl acetate with 1% acetic acid to deliver **3** followed by 1:1 *n*-hexane/ethyl acetate with 2% acetic acid to deliver **P10** (84% overall yield: 67% yield of **3** and 33% yield of **P10**).

3. Mp 131−134 °C. IR (neat, selected peaks) 1743.56, 1675.52 cm^{-1}. MS (ESI) *m/z*: 252.15 [M^+]. ^{1}H NMR (DMSO-d_6): δ 7.55 (d, J = 8.0, 2H), 7.40 (m, 2H), 7.17 (d, J = 8.4, 1H), 4.72 (s, 2H), 1.42 (s, 9H). ^{13}C NMR (DMSO-d_6): δ 167.8, 167.0, 157.7, 132.2, 129.8, 122.1, 119.5, 114.6, 81.6, 65.1, 27.7. Anal. Calcd for $C_{13}H_{16}O_5$: C, 61.90; H, 6.39; O, 31.71. Found: C, 61.61; H, 6.34; O, 32.05.

P10. Mp 203−205 °C. IR (neat, selected peaks) 1704.40 cm^{-1} (two peaks coalescing). MS (ESI) *m/z*: 196.34 [M^+]. ^{1}H NMR (DMSO-d_6): δ 7.58 (d, J = 7.2, 1H), 7.39−7.44 (m, 2H), 7.17−7.19 (d, J = 8.0, 1H), 4.76 (s, 2H). ^{13}C NMR (DMSO-d_6): δ 170.2, 167.1, 157.8, 132.2, 129.8, 122.1, 119.5, 114.6, 64.6. Anal. Calcd for $C_9H_8O_5$: C, 55.11; H, 4.11; O, 40.78. Found: C, 54.99; H, 4.22; O, 40.79.

Method B: Synthesis of 3-(2-*tert*-Butoxy-2-oxoethoxy)benzoic Acid (3). Compound **P10** (3.65 g, 18.6 mmol) was dissolved in acetonitrile (25 mL), and DMAP (227 mg, 1.86 mmol) was added. The reaction mixture was placed under nitrogen and cooled in an ice bath. Di-*tert*-butyl dicarbonate (6.10 g, 27.9 mmol) dissolved in acetonitrile (25 mL) was added via syringe, and the reaction mixture was allowed to stir overnight during which time the ice bath expired. The reaction mixture was concentrated by rotary evaporation, and the resulting red-brown oil was purified by silica gel column purification (3:1 *n*-hexane/ethyl acetate with 1% acetic acid) to yield **3** as a white powder (3.75 g, 80% yield; data as listed above).

Synthesis of Methyl 2-(3-Carbamoylphenoxy)acetic Acid (4). Rink amide MBHA (2 g, 0.5 mmol/g loading capacity) resin was weighed into a plastic column and swollen in DMF for 2 h, after which the DMF was drained, 20% piperidine in DMF was added to the resin, and the column was rotated for 10 min two times. After the resin was washed with DMF (2×), water (3×), MeOH (3×), DCM (5×), and DMF (2×), compound **3** (3 equiv), HOBt

(3.5 equiv), and DIC (3.5 equiv) were added. When the Kaiser test was negative, a cleavage mixture of TFA, H_2O, and TIS (95, 2.5, 2.5, v/v/v) were added to the resin and the column was rotated for 2 h, after which the filtrate was drained and collected. The TFA was evaporated under a constant stream of nitrogen, and the crude product was precipitated with ether and cooled in a refrigerator overnight, after which the ether−crude mixture was centrifuged, the ether decanted, and the remaining solid dissolved in acetonitrile and the process was repeated. Once finished, the product was decanted, dried by vacuum, and used without further purification (143 mg, 73.3% yield). IR (neat, selected peaks) 3455.94, 3417.96, 1723.07, 1647.11 cm^{-1}. MS (ESI) *m/z*: 196.10 [M + H^+]. ^1H NMR (DMSO-d_6): δ 13.04 (s, 1H), 7.97 (s, 1H), 7.33−7.48 (m, 4H), 7.05−7.07 (dd, J = 2.4, 8.0, 1H), 4.72 (s, 2H). ^{13}C NMR (DMSO-d_6): δ 170.1, 167.4, 157.7, 135.6, 129.3, 120.2, 117.5, 113.2, 64.5. Anal. Calcd for $C_9H_9NO_4$: C, 55.39; H, 4.65; N, 7.18; O, 32.79. Found: C, 55.30; H, 4.65; N, 7.10; O, 32.95.

Synthesis of 2-(3-(5-Acetamido-6-amino-6-oxohexylcarbamoyl)phenoxy)acetic Acid (5). Rink amide MBHA (250 mg, 0.5 mmol/g loading capacity) resin was weighed into a plastic column and swollen in DMF for 2 h, after which the DMF was drained, 20% piperidine in DMF was added to the resin, and the column was rotated for 10 min two times. After washing the resin with DMF (2×), water (3×), MeOH (3×), DCM (5×), and DMF (2×), Fmoc-Lys(Dde)-OH (3 equiv), HOBt (3.5 equiv), and DIC (3.5 equiv) were added and the column was rotated until the Kaiser test was negative. The resin was washed according to the procedure outlined above, and the Fmoc group was removed. After the wash, acetic anhydride (10 equiv) and DIEA (12 equiv) in DMF were added to the resin. After the Kaiser test was negative, the resin was washed and compound **3** (3 equiv), HOBt (3.5 equiv), and DIC (3.5 equiv) were added. When the Kaiser test was negative, a cleavage mixture of TFA, H_2O, and TIS (95, 2.5, 2.5, v/v/v) was added to the resin and the column was rotated for 2 h, after which the filtrate was drained and collected. The TFA was evaporated under a constant stream of nitrogen. The crude product was precipitated with ether and cooled in a refrigerator overnight, after which the ether−crude mixture was centrifuged. Once finished, the product was purified by reversed-phase HPLC (38 mg, 84% yield). IR (neat, selected peaks) 3460.69, 3323.01, 3308.77, 1723.07, 1613.87 cm^{-1}. MS (ESI) *m/z*: 366.17 [M + H^+]. ^1H NMR (DMSO-d_6): δ 8.42 (t, J = 5.6, 1H), 7.87 (d, J = 8.0, 1H), 7.31−7.41 (m, 4H), 7.01−7.04 (d, J = 8.4, 1H), 6.93 (s, 1H), 4.70 (s, 2H), 4.09−4.14 (m, 1H), 3.16−3.21 (q, J = 6.4, 2H), 1.80 (s, 3H), 1.57−1.64 (m, 2H), 1.43−1.49 (m, 2H), 1.25−1.31 (m, 2H). ^{13}C NMR (DMSO-d_6): δ 174.0, 170.1, 169.2, 165.6, 157.7, 136.0, 129.4, 119.9, 117.3, 113.0, 64.5, 52.3, 40.1, 31.8, 28.9, 23.0, 22.6. Anal. Calcd for $C_{17}H_{23}N_3O_6$: C, 55.88; H, 6.34; N, 11.50; O, 26.27. Found: C, 55.81; H, 6.35; N, 11.61; O, 26.23.

Synthesis of Methyl *tert*-Butyl 2-(3-formylphenoxy)acetate (6). *m*-Hydroxybenzaldehyde (10.0 g, 81.9 mmol) was dissolved in THF (70 mL), and to this solution was added K_2CO_3 (33.9 g, 245.7 mmol). The mixture was placed under nitrogen, allowed to stir for 1 h, and then cooled in an ice bath, and *tert*-butyl 2-bromoacetate (19.1 g, 98.3 mmol) was added via syringe. The solution was removed from the ice bath and warmed to room temperature, at which time TLC indicated the reaction had gone to completion. The solvent was removed by rotary evaporation. The resulting solid was dissolved in water (50 mL) and extracted with ethyl acetate (3 × 100 mL). The combined organic layers were dried with $MgSO_4$ and concentrated by rotary evaporation. The crude product (**2**) was used without further purification as a yellow solid (18.1 g, 93.5% crude yield, purity ∼98%). IR (neat, selected peaks) 1739.49, 1698.50 cm^{-1}. MS (ESI) *m/z*: 267.15 [M + H^+]. ^1H NMR (DMSO-d_6): δ 9.97 (s, 1H), 7.52−7.55 (m, 2H), 7.36−7.37 (d, J = 7.8, 1H), 7.26−7.27 (m, 1H), 4.76 (s, 2H), 1.42 (s, 9H). ^{13}C NMR (DMSO-d_6): δ 192.8, 167.6, 158.2, 137.5, 130.4, 123.1, 121.4, 113.6, 81.6, 65.1, 27.7. Anal. Calcd for $C_{13}H_{16}O_4$: C, 66.09; H, 6.83; O, 27.09. Found: C, 66.02; H, 6.89; O, 27.09.

Synthesis of 2-(3-((5-Acetamido-6-amino-6-oxohexylamino)-methyl)phenoxy)acetic Acid (7). Rink amide MBHA (250 mg, 0.5 mmol/g loading capacity) resin was weighed into a plastic column and swollen in DMF for 2 h, after which the DMF was drained, 20% piperidine in DMF was added to the resin, and the column was rotated for 10 min two times. After the resin was washed with DMF (2×), H_2O (3×), MeOH (3×), DCM (5×), and DMF (2×), Fmoc-Lys(Dde)-OH (3 equiv), HOBt (3.5 equiv), and DIC (3.5 equiv) were added and the column was rotated until the Kaiser test was negative. The resin was washed according to the procedure outlined above, and the Fmoc group was removed. After washing, acetic anhydride (10 equiv) and DIEA (12 equiv) in DMF were added to the resin. After the Kaiser test was negative, the resin was washed, compound **4** (10 equiv) dissolved in TMOF was added, and the column was rotated for 30 min. After this was added $NaCNBH_3$ (12 equiv) followed by acetic acid (100 μL). This reaction mixture was rotated in the column for 1 h, after which the Kaiser test was negative and the chloranil test was positive. A cleavage mixture of TFA, H_2O, and TIS (95, 2.5, 2.5, v/v/v) was added to the resin and the column was rotated for 2 h, after which the filtrate was drained and collected. The TFA was evaporated under a constant stream of nitrogen and the crude product was precipitated with ether and cooled in a refrigerator overnight, after which the ether−crude mixture was centrifuged. Once finished, the product was purified by reversed-phase HPLC (38 mg, 84% yield). IR (neat, selected peaks) 3318.26, 3304.02, 3194,83, 2928.96, 2857.75, 1661.35 (two peaks coalescing), 1547.41 cm^{-1}. MS (ESI) *m/z*: 352.03 [M + H^+]. ^1H NMR (DMSO-d_6): δ 8.73 (s, 1H), 7.93 (s, 2H), 6.95−7.07 (m, 4H), 4.70 (s, 2H), 4.10 (m, 1H), 3.35 (s, 2H), 2.88 (s, 1H), 2.08 (q, J = 3.2, 2H), 1.84 (s, 3H), 1.60 (m, 2H), 1.48 (m, 2H), 1.23−1.28 (m, 2H). ^{13}C NMR (DMSO-d_6): δ 173.7, 170.0, 169.2, 157.8, 133.4, 129.9, 122.3, 116.0, 114.6, 64.3, 51.9, 49.8, 46.5, 31.4, 25.0, 22.6. Anal. Calcd for $C_{17}H_{25}N_3O_5$: C, 58.11; H, 7.17; N, 11.96; O, 22.77. Found: C, 58.19; H, 7.21; N, 12.02; O, 22.58.

Mass-Tag Encoded Peptide Library Synthesis. Synthesis of the encoded peptide library was initiated by swelling Tentagel beads (5 g, 90 μm capacity, 0.27 mmol/g) in a 60 mL plastic column in water (50 mL) for 48 h. The water was drained, and the beads were transferred to a glass reaction vessel (250 mL capacity) with a sintered glass filter frit. A solution of DCM/ether (45:55, 100 mL) was added to the beads, and Alloc-OSu (0.1 equiv), dissolved in DCM/ether (45:55, 50 mL), was added to the suspended resin beads. DIEA (2 equiv) was added to the solution and the glass container was then shaken vigorously for 30 min, after which the solution was drained and the beads were transferred back to the 60 mL plastic column. The beads were swollen in DMF for 2 h, and the cleavable linker was assembled according standard Fmoc peptide chemistry with the following reagents: Fmoc-Met-OH (3 equiv), Fmoc-Arg(Pmc)-OH (3 equiv), *N*-Fmoc-3-(4-bromophenyl)-β-alanine, *N*-Fmoc-2,2′-ethylenedioxybis(ethylamine) monosuccinamide (3 equiv). All coupling reactions were performed in DMF (50 mL) with the standard coupling reagents HOBt (3.5 equiv) and DIC (3.5 equiv). All Fmoc deprotections were performed with 20% piperidine in DMF (45 mL). After each reaction step, the beads were washed with DMF, water, methanol, and DCM (5 × 35 mL each). Following these reactions, the column containing the beads was subjected to Alloc deprotection using tetrakis(tirphenylphosphine)palladium(0) (0.2 equiv) and phenylsilane (20 equiv) in DCM for 30 min. After this time, the solution was drained, a fresh solution of the same reagents was added, and the column was rotated for another 30 min. The Fmoc group on the cleavable linker was removed next with 20% piperidine in DMF (45 mL) for 20 min. The resulting resin beads were then equally distributed into 48 plastic columns (2 mL) secured in a Teflon block. One of the Fmoc protected amino acid diversity elements (3 equiv) and HOBt (3,5 equiv) in DMF (1.5 mL) and DIC (3.5 equiv) were added to each column. The Teflon block was then placed on a shaker, and the reactions were allowed to proceed for 3 h. Once all Kaiser tests were negative for each column, the beads were pooled and the Fmoc protecting group was removed. Semiorthogonally protected Fmoc-Lys(Dde)-OH (3 equiv) was coupled using HOBt and DIC (3.5 equiv each). Once the coupling was complete, the Fmoc group was

removed and the beads were washed with DMF, water, methanol, and DCM (5 × 35 mL each) and then dried completely under vacuum for 1 day. When dry, the beads were reswollen in water for 24 h. The beads were once again transferred to a glass reaction vessel with a filter frit. An amount of 100 mL of the DCM/ether solution (45:55) solution was added followed by Fmoc-OSu (0.7 equiv) dissolved in the DCM/ether solution (50 mL). DIEA (2 equiv) was added to the column and it was shaken vigorously for 30 min, after which the solution was drained and the beads were transferred back to a 60 mL plastic column. $(Boc)_2O$ (0.6 equiv) in DIEA (1.2 equiv) was added, and the reaction was allowed to proceed until a Kaiser test of the beads was negative. The Fmoc protecting group was then removed, and the beads were distributed evenly to 48 plastic columns (2 mL) secured in a Teflon block. One of the carboxylic acid diversity elements (10 equiv) and HOBt (15 equiv) in DMF (1.5 mL) along with DIC (15 equiv) were added to each column. The Teflon block was placed in a shaker, and the reactions were allowed to proceed for 16 h, after which a Kaiser test was performed on each column. All results were negative. The beads were pooled and washed with DMF, water, methanol, DCM, and DMF (5 × 35 mL). Next, the Dde group was removed using 2% hydrazine in DMF (40 mL. reaction repeated twice) and compound **3** (5 equiv) was coupled to the beads using HOBt (7.5 equiv) in DMF (40 mL) and DIC (7.5 equiv). When the reaction was complete, deprotection of all remaining protecting groups was performed with 45 mL of 82.5% TFA, 5% phenol, 5% thioanisole, 5% H_2O, and 2.5% TIS and rotation for 2 h. After the final deprotection, the beads were neutralized with DIEA in DMF and then washed thoroughly with DMF, water, methanol, and DCM (5 × 40 mL each), dried, and stored in a vacuum desiccator for future use.

COPAS Sorting of the Peptide Library. The mass-tag encoded peptide library was hydrated in water, transferred to the COPAS instrument, diluted with a solution of PBS containing 0.2% Tween-20, 0.05% NaN_3, and 0.1% BSA (PBSTBN), then sorted with the lens tuned to emit at 488 and 605 nm, and detected by a green and red photomultiplier tube, respectively. An initial sort of beads (2300 beads) defined the main cluster of autofluorescence for the library of beads. On the basis of this established base of autofluorescence, a threshold was chosen that allowed the COPAS instrument to divert beads with strong autofluorescence from the majority of the beads with low autofluorescence. The beads were sorted at this fluorescence level several times in batches of 5000−25000 beads per batch.

Library Prescreening, Screening, and Isolation of Hits. Tentagel beads (approximately 3000−4000) containing the target peptide library were swollen in 1 mL of buffer A (50 mM bicine [pH 8.5], 1 mM DTT, 50 mM KCl, 0.2% Tween-20, 0.1% gelatin) for 60 min. The enzyme solution used for bead screening contained 0.31 nM Alexa Fluor 488 labeled ADCS in buffer A. The beads were then incubated with 1 mL of abeled ADCS for 60 min at room temperature. The incubation solutions were visualized under a fluorescence microscope fitted with a long-band green filter. The brightest beads were isolated manually with a pipet tip.

Cleavage of the Resin Beads for MALDI-TOF MS Analysis. Beads isolated for library synthesis checks were washed with water and then transferred to a 250 μL polypropylene microcentrifuge tube in water with the help of a microscope. Beads isolated from library screenings in the presence of ADCS were washed with water and 8 M guanidine HCl in succession three times for 5 min in each cycle. One final washing was done with water, and the individual beads were transferred to a 250 μL polypropylene microcentrifuge tube containing water with the help of a microscope. After transfer to the polypropylene tube, MALDI-TOF MS analysis was performed on each compound according to the following procedure. Cyanogen bromide (20 mg/mL) in 70% formic acid was added (30 μL) to each bead-containing tube. The tube was sealed and left overnight at room temperature. The tube was then lyophilized to dryness. A water/acetonitrile (45:55, 70 μL) solution with 0.1% TFA was added to each tube, and 0.7 μL of this solution was mixed with an equal volume of a saturated solution of an α-cyano-4-hydroxycinnamic acid solution in water/acetonitrile (45:55) solution with 0.1% TFA on a MALDI-TOF target and allowed to evaporate to dryness. This target was then inserted into the MALDI-TOF MS instrument, and the samples were analyzed in reflectron mode.

Resynthesis and Characterization of Peptides. Larger-scale resynthesis of the peptides identified as ADCS binders was performed on 100 mg of Fmoc Rink MHBA amide resin (capacity, 0.65 mmol/g) contained in a 1 mL plastic column. The beads were swollen in DMF for 60 min, drained, and then treated with 3 mL of 25% piperidine in DMF twice, first for 5 min and next for 15 min. After Fmoc deprotection, the beads were washed with DMF (5 × 0.8 mL) and the peptide sequence was constructed using the appropriate amino (3 equiv) and carboxylic acids (10 equiv) along with HOBt and DIC (13 equiv each). The target peptide was cleaved from the resin using 0.9 mL of 95% TFA, 2.5% H_2O, and 2.5% TIS for 2 h. The cleavage solution was collected and concentrated by evaporation, and 5−10 mL ether was added until the product had completely precipitated. The filtrate was cooled to −80 °C for 14 h and centrifuged. The precipitated product was dried under vacuum for 24 h and then purified by HPLC. Collected fractions were lyophilized, and the resulting solids were subjected to HPLC and ES-MS analysis (see Supporting Information for details).

Enzyme Preparation, Assay, and Labeling. The *pabA, pabB,* and *pabC* genes encoding PabA, ADCS, and ADCL, respectively, were amplified from *Escherichia coli* K12 chromosomal DNA. The *pabA* gene was cloned into a pET3a (Novagen) vector using *Nde*I and *BamH*I restriction sites. *pabB* and *pabC* genes were cloned into a pET28a vector (Novagen) using *Nde*I and *BamH*I restriction sites for expression as a 6×His-tagged fusion protein.

PabA was overexpressed by *E. coli* BL21 (DE3) Gold cells grown in TB medium after induction by 0.5 mM IPTG at OD_{600} = 0.6. Cells were harvested by centrifugation and resuspended in lysis buffer (100 mM TEA, pH 7.8, 30 mM mercaptoethanol, 1 mM EDTA, 0.5 mg/mL lysozyme, 0.2 units/mL DNase I) prior to disruption by sonication. Cell debris was pelleted by centrifugation at 14 000 rpm, and a 15−40% ammonium sulfate fractionation was performed. The 40% precipitate was dissolved in a minimum volume of starting buffer (50 mM TEA, pH 7.8, 10 mM mercaptoethanol, 5 mM $MgCl_2$, 1 mM EDTA) and loaded onto a Q-Sepharose fast flow column. Protein was eluted with a linear gradient of 500 mL of 0−300 mM KCl in starting buffer. Fractions were concentrated by ultrafiltration and dialyzed against 20 mM KP_i, pH 7.5, 50 mM KCl, and 1 mM DTT. Purified enzyme was flash-frozen and stored at −80 °C. Protein concentration was measured with the Bio-Rad DC assay, using IgG as standard. Yield was ∼83 mg of purified protein per 21 g of cell paste.

PabB was overexpressed in *E. coli* BL21 (DE3) Gold cells grown in TB medium with induction by 0.5 mM IPTG at OD_{600} = 0.6. Cells were harvested by centrifugation and resuspended in lysis buffer (20 mM Na_2HPO_4, pH 7.4, 500 mM NaCl, 1 mM mercaptoethanol, 10 mM imidazole, 0.5 mg/mL lysozyme, 0.2 units/mL DNase I) prior to disruption by sonication. Cell debris was pelleted by centrifugation at 14 000 rpm, and the supernatant was incubated at room temperature for 30 min with chelating Sepharose fast flow resin (Pharmacia) that was charged with Ni^{2+}. Resin-bound protein was eluted with a linear gradient of 10−300 mM imidazole in starting buffer (20 mM Na_2HPO_4, pH 7.4, 500 mM NaCl, 1 mM mercaptoethanol, 10 mM imidazole). Concentration, dialysis, and storage conditions were as described for PabA. Yield was ∼185 mg of purified protein per 5 g of cell paste.

PabC preparation was the same as for PabB except that 20 μM PLP was included in the lysis, starting, and dialysis buffers. Yield was ∼460 mg of purified protein per 37 g of cell paste.

ADCS and the lysine-reactive green fluorescence dye Alexa Fluor 488 (Molecular Probes) were mixed in a 1:50 ratio in 0.2 M sodium bicarbonate solution, pH 8.4. This mixture was incubated in the dark at room temperature for 1.5 h in the presence of 1 mM DTT. Unreacted dye molecules were separated from ADCS by using Sephadex G25 spin columns. The extent of labeling was ∼1 dye per ADCS.

All kinetic assays were performed on a Kontron Uvikon 930 UV−vis spectrophotometer at 25 °C. Reactions of mixtures

containing inhibitors were followed by the disappearance of NADH in a coupled assay with excess ADCL and LDH. Each 500 μL of mixture consisted of 100 mM bicine, pH 8.5, 20 mM L-glutamine, 5 mM $MgCl_2$, 20 μM PLP, 7 μM ADCL, 200 μM NADH, 13 μM chorismate, 2 units of LDH, 0.5 μM PabA, and 0.5 μM ADCS.

For K_i determinations, inhibitors were dissolved in water and brought to pH 9 with 25 mM NaOH. Inhibitor concentrations were varied from 200 to 1000 μM, while the chorismate concentration was held constant. Reaction mixtures were incubated for 5 min at 25 °C prior to reaction initiation by an equimolar solution of PabA and ADCS. K_i values were determined by fitting initial rate data to eq 1.

The ordered binding kinetic data were collected by monitoring the increase in absorbance at 290 nm, due to formation of PABA, in a coupled assay with excess ADCL. Each 500 μL of mixture contained 100 mM bicine, pH 8.5, 20 mM L-glutamine, 20 μM PLP, 7 μM ADCL, 0.5 μM PabA, and 0.5 μM ADCS. Chorismate concentration was varied from 50 to 650 μM, and Mg^{2+} concentration was varied from 15 to 450 μM. Reaction mixtures were incubated for 5 min at 25 °C prior to reaction initiation by an equimolar solution of PabA and ADCS. To determine $K_{chorismate}$ and $K_{Mg^{2+}}$, a saturation curve for each substrate was obtained. Magnesium concentration was held constant at 15 μM, and chorismate concentration varied from 50 to 825 μM. Chorismate concentration was held constant at 500 μM, and magnesium concentration varied from 5 to 750 μM.

Acknowledgment. We thank the National Science Foundation (Grant CHE-0313888) for financial support, as well as Scott Eaton, Wren Yahraus, and Michael Descilletes for helpful discussions.

Supporting Information Available: Figures S1 (fluorescence images of the on-bead library) and S2 (model of **5** bound to ADCS with the PAYLOAD in the active site); ^{1}H NMR and ^{13}C NMR spectra for molecules **1**−**3**, **P10**, and **4**−**7**; experimental procedures and ^{1}H NMR and ^{13}C NMR data for **P1** and **P8**; structures of amino acid and carboxylic acid diversity elements used in the library synthesis; MALDI-TOF MS results of encoding tags cleaved during the synthesis of the library and selected identified compounds; MALDI-TOF mass spectra for **L1**, **L3**, **L5**, and **L9**; ESI-MS data, MS spectra, purity data, and HPLC traces for **L1**−**L11**, **L3** linker, and **L5** linker. This material is available free of charge via the Internet at http://pubs.acs.org.

References

(1) Easson, M. A. M.; Rees, D. C. Combinatorial chemistry: tools for the medicinal chemist. *Med. Chem. (Wiley)* **2002**, 359−381.
(2) Thompson, L. A.; Ellman, J. A. Synthesis and applications of small molecule libraries. *Chem. Rev.* **1996**, *96* (1), 555−600.
(3) Lee, A.; Breitenbucher, J. G. The impact of combinatorial chemistry on drug discovery. *Curr. Opin. Drug Discovery Dev.* **2003**, *6* (4), 494−508.
(4) Furka, A.; Sebestyen, F.; Asgedom, M.; Dibo, G. General method for rapid synthesis of multicomponent peptide mixtures. *Int. J. Pept. Protein Res.* **1991**, *37* (6), 487−493.
(5) Lam, K. S.; Salmon, S. E.; Hersh, E. M.; Hruby, V. J.; Kazmierski, W. M.; Knapp, R. J. A new type of synthetic peptide library for identifying ligand-binding activity. *Nature* **1991**, *354* (6348), 82−84.
(6) Houghten, R. A.; Pinilla, C.; Blondelle, S. E.; Appel, J. R.; Dooley, C. T.; Cuervo, J. H. Generation and use of synthetic peptide combinatorial libraries for basic research and drug discovery. *Nature* **1991**, *354* (6348), 84−86.
(7) Lam, K. S.; Lebl, M.; Krchnak, V. The "one-bead-one-compound" combinatorial library method. *Chem. Rev.* **1997**, *97* (2), 411−448.
(8) Dixon, S.; Wang, X.; Lam, K. S.; Kurth, M. J. Solid-phase synthesis of quinoxaline, thiazine, and oxazine analogs through a benzyne intermediate. *Tetrahedron Lett.* **2005**, *46*, 7443−7446.
(9) Wang, X.; Zhang, J.; Song, A.; Lebrilla, C. B.; Lam, K. S. Encoding method for OBOC small molecule libraries using a biphasic approach for ladder-synthesis of coding tags. *J. Am. Chem. Soc.* **2004**, *126* (18), 5740−5749.
(10) Lam, K. S.; Lebl, M. *ImmunoMethods* **1992**, *1*, 11−15.
(11) Lam, K. S.; Lehman, A. L.; Song, A.; Doan, N.; Enstrom, A. M.; Maxwell, J.; Liu, R. Synthesis and screening of "one-bead one-compound" combinatorial peptide libraries. *Methods Enzymol.* **2003**, *369*, 298−322.
(12) Hwang, S.; Tamilarasu, N.; Ryan, K.; Huq, I.; Richter, S.; Still, W. C.; Rana, T. M. Inhibition of gene expression in human cells through small molecule−RNA interactions. *Proc. Natl. Acad. Sci. U.S.A.* **1999**, *96* (23), 12997−13002.
(13) Alluri, P. G.; Reddy, M. M.; Bachhawat-Sikder, K.; Olivos, H. J.; Kodadek, T. Isolation of protein ligands from large peptoid libraries. *J. Am. Chem. Soc.* **2003**, *125* (46), 13995−14004.
(14) Hu, Y.; Helm, J. S.; Chen, L.; Ginsberg, C.; Gross, B.; Kraybill, B.; Tiyanont, K.; Fang, X.; Wu, T.; Walker, S. Identification of selective inhibitors for the glycosyltransferase MurG via high-throughput screening. *Chem. Biol.* **2004**, *11* (5), 703−711.
(15) Youngquist, R. S.; Fuentes, G. R.; Lacey, M. P.; Keough, T. Matrix-assisted laser desorption ionization for rapid determination of the sequences of biologically active peptides isolated from support-bound combinatorial peptide libraries. *Rapid Commun. Mass Spectrom.* **1994**, *8* (1), 77−81.
(16) Liu, R.; Marik, J.; Lam, K. S. A novel peptide-based encoding system for "one-bead one-compound" peptidomimetic and small molecule combinatorial libraries. *J. Am. Chem. Soc.* **2002**, *124* (26), 7678−7680.
(17) Roberts, C. W.; Roberts, F.; Lyons, R. E.; Kirisits, M. J.; Mui, E. J.; Finnerty, J.; Johnson, J. J.; Ferguson, D. J.; Coggins, J. R.; Krell, T.; Coombs, G. H.; Milhous, W. K.; Kyle, D. E.; Tzipori, S.; Barnwell, J.; Dame, J. B.; Carlton, J.; McLeod, R. The shikimate pathway and its branches in apicomplexan parasites. *J. Infect. Dis.* **2002**, *185* (Suppl. 1), S25−S36.
(18) Knaggs, A. R. The biosynthesis of shikimate metabolites. *Nat. Prod. Rep.* **2003**, *20* (1), 119−136.
(19) Smith, D. A.; Parish, T.; Stoker, N. G.; Bancroft, G. J. Characterization of auxotrophic mutants of Mycobacterium tuberculosis and their potential as vaccine candidates. *Infect. Immun.* **2001**, *69* (2), 1142−1150.
(20) McArthur, J. D.; West, N. P.; Cole, J. N.; Jungnitz, H.; Guzman, C. A.; Chin, J.; Lehrbach, P. R.; Djordjevic, S. P.; Walker, M. J. An aromatic amino acid auxotrophic mutant of Bordetella bronchiseptica is attenuated and immunogenic in a mouse model of infection. *FEMS Microbiol. Lett.* **2003**, *221* (1), 7−16.
(21) Trias, J. The role of combichem in antibiotic discovery. *Curr. Opin. Microbiol.* **2001**, *4* (5), 520−525.
(22) Istvan, E. S.; Deisenhofer, J. Structural mechanism for statin inhibition of HMG-CoA reductase. *Science* **2001**, *292* (5519), 1160−1164.
(23) Maly, D. J.; Choong, I. C.; Ellman, J. A. Combinatorial target-guided ligand assembly: identification of potent subtype-selective c-Src inhibitors. *Proc. Natl. Acad. Sci. U.S.A.* **2000**, *97* (6), 2419−2424.
(24) Szczepankiewicz, B. G.; Liu, G.; Hajduk, P. J.; Abad-Zapatero, C.; Pei, Z.; Xin, Z.; Lubben, T. H.; Trevillyan, J. M.; Stashko, M. A.; Ballaron, S. J.; Liang, H.; Huang, F.; Hutchins, C. W.; Fesik, S. W.; Jirousek, M. R. Discovery of a potent, selective protein tyrosine phosphatase 1B inhibitor using a linked-fragment strategy. *J. Am. Chem. Soc.* **2003**, *125* (14), 4087−4096.
(25) Song, A.; Zhang, J.; Lebrilla, C. B.; Lam, K. S. A novel and rapid encoding method based on mass spectrometry for "one-bead−one-compound" small molecule combinatorial libraries. *J. Am. Chem. Soc.* **2003**, *125* (20), 6180−6188.
(26) Dixon, S. M.; Li, P.; Liu, R.; Wolosker, H.; Lam, K. S.; Kurth, M. J.; Toney, M. D. Slow-binding human serine racemase inhibitors from high-throughput screening of combinatorial libraries. *J. Med. Chem* **2006**, *49*, 2388−2397.
(27) George, J.; Teear, M. L.; Norey, C. G.; Burns, D. D. Evaluation of an imaging platform during the development of a FRET protease assay. *J. Biomol. Screening* **2003**, *8* (1), 72−80.
(28) Mehrotra, M. M.; Heath, J. A.; Rose, J. W.; Smyth, M. S.; Seroogy, J.; Volkots, D. L.; Ruhter, G.; Schotten, T.; Alaimo, L.; Park, G.; Pandey, A.; Scarborough, R. M. Spirocyclic nonpeptide glycoprotein IIb-IIIa antagonists. Part 3: synthesis and SAR of potent and specific 2,8-diazaspiro[4.5]decanes. *Bioorg. Med. Chem. Lett.* **2002**, *12* (7), 1103−1107.
(29) DeVries, V. G.; Largis, E. E.; Miner, T. G.; Shepherd, R. G.; Upeslacis, J. Potential antiatherosclerotic agents. 4. [(Functionalized-alkyl)amino]benzoic acid analogues of cetaben. *J. Med. Chem.* **1983**, *26* (10), 1411−1421.
(30) Lu, Z.; Tweig, R. J. Copper-catalyzed aryl amination in aqueous media with 2-dimethylaminoethanol ligand. *Tetrahedron Lett.* **2005**, *46* (17), 2997−3001.
(31) Zhang, X.; Dillen, L.; Vanhoutte, K.; Van Dongen, W.; Esmans, E.; Claeys, M. Characterization of unstable intermediates and oxidized products formed during cyanogen bromide cleavage of peptides and proteins by electrospray mass spectrometry. *Anal. Chem.* **1996**, *68*, 3422−3430.

(32) Yue, W.; Koen, Y. M.; Williams, T. D.; Hanzlik, R. P. Use of isotopic signatures for mass spectral detection of protein adduction by chemically reactive metabolites of bromobenzene: Studies with model proteins. *Chem. Res. Toxicol.* **2005**, *18*, 1748−1754.
(33) Tornoe, C. W.; Sanderson, S. J.; Mottram, J. C.; Coombs, G. H.; Meldal, M. Combinatorial library of peptidotriazoles: identification of [1,2,3]-triazole inhibitors against a recombinant Leishmania mexicana cysteine protease. *J. Comb. Chem.* **2004**, *6* (3), 312−324.
(34) Carniel, E. The Yersinia high-pathogenicity island: an iron-uptake island. *Microbes. Infect.* **2001**, *3* (7), 561−569.
(35) Budzikiewicz, H. Siderophores of the human pathogenic fluorescent pseudomonads. *Curr. Top. Med. Chem.* **2001**, *1* (1), 1−6.
(36) Payne, R. J.; Toscano, M. D.; Bulloch, E. M.; Abell, A. D.; Abell, C. Design and synthesis of aromatic inhibitors of anthranilate synthase. *Org. Biomol. Chem.* **2005**, *3* (12), 2271−2281.
(37) Kozlowski, M. C.; Tom, N. J.; Seto, C. T.; Sefler, A. M.; Bartlett, P. A. Chorismate-utilizing enzymes isochorismate synthase, anthranilate synthase, and *p*-aminobenzoate synthase: mechanistic insight through inhibitor design. *J. Am. Chem. Soc.* **1995**, *117* (8), 2128−2140.
(38) Morollo, A. A.; Eck, M. J. Structure of the cooperative allosteric anthranilate synthase from Salmonella typhimurium. *Nat. Struct. Biol.* **2001**, *8* (3), 243−247.
(39) He, Z.; Stigers Lavoie, K. D.; Bartlett, P. A.; Toney, M. D. Conservation of mechanism in three chorismate-utilizing enzymes. *J. Am. Chem. Soc.* **2004**, *126* (8), 2378−2385.
(40) Walsh, C. T.; Erion, M. D.; Walts, A. E.; Delany, J. J., 3rd; Berchtold, G. A. Chorismate aminations: partial purification of Escherichia coli PABA synthase and mechanistic comparison with anthranilate synthase. *Biochemistry* **1987**, *26* (15), 4734−4745.

JM0609869